


Estimator of entropy production for partially accessible Markov networks based on the observation of blurred transitions

Benjamin Ertel  and Udo Seifert 

II. Institut für Theoretische Physik, Universität Stuttgart, 70550 Stuttgart, Germany

 (Received 13 December 2023; accepted 25 March 2024; published 6 May 2024)

A central task in stochastic thermodynamics is the estimation of entropy production for partially accessible Markov networks. We establish an effective transition-based description for such networks with transitions that are not distinguishable and therefore blurred for an external observer. We demonstrate that, in contrast to a description based on fully resolved transitions, this effective description is typically non-Markovian at any point in time. Starting from an information-theoretic bound, we derive an operationally accessible entropy estimator for this observation scenario. We illustrate the operational relevance and the quality of this entropy estimator with a numerical analysis of various representative examples.

DOI: [10.1103/PhysRevE.109.054109](https://doi.org/10.1103/PhysRevE.109.054109)

I. INTRODUCTION

One major result of stochastic thermodynamics is the identification of entropy production for physical systems within a Markovian description [1–3]. Based on this identification, the dissipation in chemical and biophysical systems, for instance chemical reaction networks [4–6], can be quantified theoretically. In practice, however, many systems are only partially accessible, i.e., the full Markovian description is not observed, implying that the entropy production is not directly operationally accessible.

For inferring the entropy production of these partially accessible systems, various strategies with different level of sophistication have been proposed. The apparent entropy production [7–10] and state-lumping entropy estimators [11–15] bound the full entropy production with the coarse-grained entropy production of effective Markov models. Time-series estimators [16,17] and fluctuation theorem estimators [18–20] provide entropy bounds based on the irreversibility of time-antisymmetric observables. The thermodynamic uncertainty relation can be interpreted as a bound for the entropy production in terms of current fluctuations [21–25]. As shown in Ref. [26], the statistics of general counting observables bound the entropy production as well. Assuming a specific underlying Markov network, optimization procedures yield tight network specific entropy bounds [27–30].

Including waiting times in the effective description, for example, via the milestone coarse-graining scheme [31,32], leads to more refined entropy estimators with a broader range of applicability [33–38]. In particular, the effective description based on the waiting times between two observable transitions is central for thermodynamic inference as it provides a tight entropy bound [39,40] and additionally contains topological information about the underlying system [39,41–44]. This inference strategy is based on interpreting the observed transitions as renewal events of an effective semi-Markov description [45–47] and identifying these renewal events as Markovian events [48,49].

In realistic scenarios, e.g., the scenarios discussed in Ref. [50], imperfect measurements can limit the resolution of observations resulting in non-Markovian events. For an example, consider the observation of a chemical reaction network. Instead of observing the precise number of each chemical species, an external observer can potentially only register the type of an observed reaction. Consequently, the individual transitions in the state space are not distinguishable. Stated differently, for this observer, the transitions of the corresponding effective Markov network are blurred. This blurred observation of a chemical reaction network is illustrated in Fig. 1 for the Schlögl model, a paradigmatic example of a chemical reaction network [51–54].

A biophysical example with blurred transitions is an observation of the KaiC-cycle [55–58] in which the observer only registers activation and deactivation of KaiC molecules but cannot distinguish between the different molecular states. An example from active matter is an observation of the motion of a run-and-tumble particle subject to thermal noise [59–61] in which the orientations of the director are not accessible and therefore blurred. Another example is an observation of a quantum-dot system [7,62–65] with multiple indistinguishable reservoirs as introduced in Ref. [66]. Since the observer cannot distinguish which reservoir populates or depletes the system, the corresponding transitions are blurred. Note that from a conceptual point of view, the multifilar events introduced in Ref. [66] correspond to blurred transitions.

This work aims at extending the transition-based description of partially accessible Markov networks to this class of observations. Based on an information-theoretic bound, we derive an operationally accessible entropy estimator which uses blurred transition statistics and the distributions of waiting times between two consecutive blurred transitions. Crucially, the derived estimator is not the generalization of the entropy estimator for fully resolved transitions since the Markovian event property breaks down for blurred transitions.

We start with a recapitulation of the basic concepts of transition-based thermodynamic inference for resolved

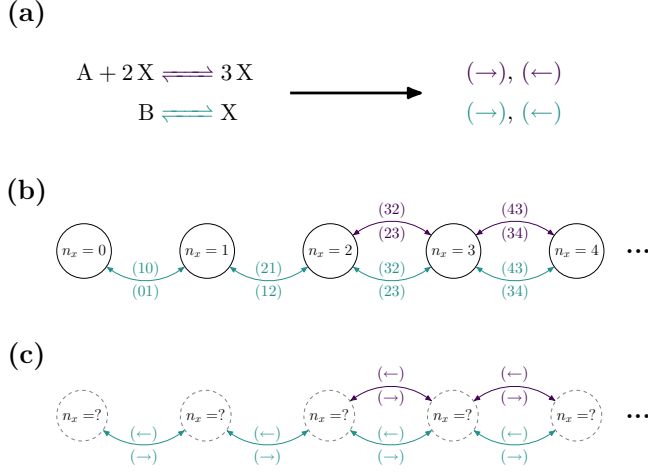


FIG. 1. Blurred observation of the Schlögl model. (a) Reaction scheme: X molecules can undergo chemical reactions with A molecules and B molecules provided by two different chemical reservoirs. (b) If an observer resolves the number of X molecules n_X , each change in n_X can be represented as transition in an effective Markov network with two different channels. (c) If the observer only registers forward and backward reactions along the A -reaction channel (dark color) or the B -reaction channel (bright color) but cannot resolve the changes in the number of X molecules n_X , the corresponding transitions of the effective network are blurred for this observer.

transitions in Sec. II. These concepts are extended to blurred transitions in Sec. III. In Sec. IV, we derive the transition-based entropy estimator starting from the corresponding information-theoretic bound. Various examples illustrating the quality of this estimator are presented in Sec. V. The final Sec. VI contains a concluding perspective.

II. SETUP

A. Underlying Markovian description

Our starting point is a Markov network with N states for which transitions between state i and state j happen with a time-independent transition rate k_{ij} along a corresponding edge or, equivalently, link of the network. To ensure thermodynamic consistency, we assume that $k_{ij} > 0$ implies $k_{ji} > 0$. Since all transition rates are time-independent, the system reaches a stationary state with stationary probabilities p_i^s in the long-time limit $t \rightarrow \infty$. If the detailed balance relation $p_i^s k_{ij} = p_j^s k_{ji}$ is broken for at least one edge, this steady state is a nonequilibrium stationary state (NESS) with stationary entropy production rate

$$\langle \sigma \rangle = \sum_{ij} p_i^s k_{ij} \ln \frac{p_i^s k_{ij}}{p_j^s k_{ji}} \geq 0, \quad (1)$$

where the summation includes all possible transitions [3]. From a topological perspective, $\langle \sigma \rangle$ is caused by currents j_C along closed directed loops without self-crossing, i.e., along the cycles C of the network. Operationally, j_C corresponds to the mean net number of cycle completions divided by the observation time [67,68]. The contribution of each cycle C to the entropy production of the network is quantified by the

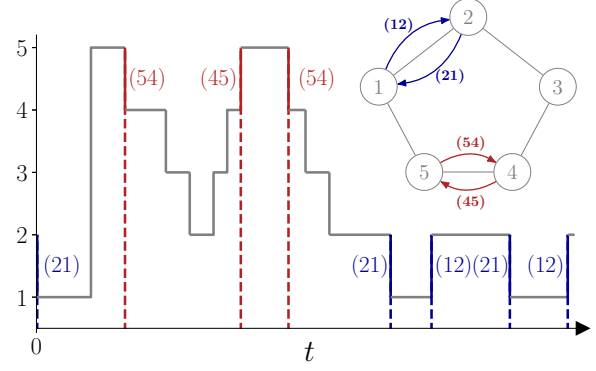


FIG. 2. Observation of a partially accessible five-state Markov network with four resolved transitions. The resolved observer registers the transitions (12), (21), (45), and (54) and the corresponding in-between waiting times.

cycle affinity

$$\mathcal{A}_C \equiv \ln \prod_{ij \in C} \frac{k_{ij}}{k_{ji}}, \quad (2)$$

where the product includes all forward transition rates of the cycle in the numerator and the corresponding backward transition rates in the denominator. Combining the contributions of all cycles of the network, $\langle \sigma \rangle$ can be calculated via

$$\langle \sigma \rangle = \sum_C j_C \mathcal{A}_C, \quad (3)$$

which is equivalent to Eq. (1). In unicyclic networks, Eq. (3) reduces to

$$\langle \sigma \rangle = j_C \mathcal{A}_C. \quad (4)$$

For this topology, the cycle current is identical to the current through each link and therefore given by

$$j_C = p_i^s k_{ij} - p_j^s k_{ji}, \quad (5)$$

where i and j can be any pair of adjacent states.

B. Resolved observation

We assume that an observer, whom we call “resolved observer” for later reference, aims at inferring $\langle \sigma \rangle$ of the general N -state Markov network based on the observation of $2M$ transitions along M different edges. In the course of time, for example during the observation of the five-state Markov network with four resolved transitions shown in Fig. 2, the observer registers different transitions and the waiting times between these transitions. This observation results in an effective dynamics for the underlying network that is characterized by waiting time distributions of the form

$$\psi_{(ij) \rightarrow (kl)}(t) \equiv p[(kl); T_{(kl)} - T_{(ij)} = t | (ij)], \quad (6)$$

where $T_{(ij)}$ is the time at which transition (ij) is registered. $\psi_{(ij) \rightarrow (kl)}(t)$ is the probability density for observing (kl) at time $T_{(kl)} = T_{(ij)} + t$, i.e., after a waiting time t , given (ij) was observed at time $T_{(ij)}$. Integrating out the waiting times

in Eq. (6) leads to

$$P_{(ij)\rightarrow(kl)} = \int_0^\infty dt \psi_{(ij)\rightarrow(kl)}(t), \quad (7)$$

which is the probability for observing the resolved transition (kl) after the resolved transition (ij) irrespective of the waiting time in between with normalization $\sum_{(kl)} P_{(ij)\rightarrow(kl)} = 1$.

In general, the emerging effective description of the network is non-Markovian because the described partial observation is not sufficient for determining the state of the underlying network. As a consequence, the corresponding waiting time distributions are typically nonexponential. However, directly after a registered transition, the state of the system is uniquely determined by this transition. For example, in Fig. 2, observing (12) implies that the state of the system directly after the transition is two. Therefore, the effective description remains Markovian at the corresponding time instances. From a conceptual point of view, these events can be interpreted as the renewal events of a semi-Markov process which describes the effective dynamics in the space of observable transitions [39]. Each observed transition updates the semi-Markov state of the system by renewing the memory of the non-Markovian process with a Markovian event. Thus, in the space of observable transitions, the process is a first-order semi-Markov process.

The updating of the semi-Markov state slices an observed trajectory into snippets starting and ending with an observed transition, i.e., a Markovian event. From an operational point of view, e.g., for the resolved observer, this slicing implies that waiting time distributions for transition sequences with more than two transitions factorize. For example, for the sequence $(ij) \rightarrow (kl) \rightarrow (mn)$ with in-between waiting times t_1 and t_2 , we have

$$\psi_{(ij)\rightarrow(kl)\rightarrow(mn)}(t_1, t_2) = \psi_{(ij)\rightarrow(kl)}(t_1) \psi_{(kl)\rightarrow(mn)}(t_2). \quad (8)$$

Since the memory is renewed at the start and at the end of each snippet, the path weight of the trajectory splits into the path weights of the corresponding subsequent trajectory snippets [39,48]. On the level of these trajectory snippets, a fluctuation theorem holds true for their path weights which relates a single snippet to the completion of paths, especially of cycles [39,48]. Based on this fluctuation theorem, the entropy estimator

$$\langle \hat{\sigma} \rangle \equiv \sum_{(ij),(kl)} \int_0^\infty dt \pi_{ij} \psi_{(ij)\rightarrow(kl)}(t) \ln \frac{\psi_{(ij)\rightarrow(kl)}(t)}{\psi_{(\tilde{k}l)\rightarrow(\tilde{i}j)}(t)} \quad (9)$$

for the full entropy production $\langle \sigma \rangle$ of a partially accessible Markov network can be derived [39,40]. In Eq. (9), the summation includes all observed transitions, $(\tilde{i}j) = (ji)$ is the time-reversed transition of (ij) and $\pi_{ij} = p_i^s k_{ij}$ is the rate for observing transition (ij) . This entropy estimator always provides a lower bound on the full entropy production, i.e., $\langle \hat{\sigma} \rangle \leq \langle \sigma \rangle$. Especially for unicyclic networks, the observation of transitions (ij) and (ji) along a single link recovers the full entropy production, i.e., $\langle \hat{\sigma} \rangle = \langle \sigma \rangle = j_C \mathcal{A}_C$, because

$$\int_0^\infty dt (\pi_{ij} \psi_{(ij)\rightarrow(ij)}(t) - \pi_{ji} \psi_{(ji)\rightarrow(ji)}(t)) = j_C \quad (10)$$

and

$$\ln \frac{\psi_{(ij)\rightarrow(ij)}(t)}{\psi_{(ji)\rightarrow(ji)}(t)} = \mathcal{A}_C \quad (11)$$

hold true [39,40].

III. FROM RESOLVED TO BLURRED OBSERVATIONS

We now assume that a second observer with finite resolution, whom we call “blurred observer” for later reference, also observes the $2M$ transitions of the underlying network. However, due to the finite resolution of his observation, this observer cannot distinguish between the $2M$ resolved transitions and instead observes C blurred transitions with $2 \leq C \leq M$. Stated differently, for the blurred observer, the resolved transitions are grouped into C different effective transition classes G, H, I, \dots with each transition belonging to one transition class. A concrete example in which the four observable transitions of the network in Fig. 2 are blurred into two transition classes is shown in Fig. 3(a). For these transitions, the blurred observer registers only the corresponding transition class but cannot distinguish between individual transitions within each class. The conditioned probability for observing a specific transition (ij) of transition class I is given by

$$p(ij|I) = \frac{p_i^s k_{ij}}{\sum_{(kl) \in I} p_k^s k_{kl}} = \frac{\pi_{ij}}{\pi_I}, \quad (12)$$

where π_I is the rate for observing that a transition within I happens and the summation includes all transitions within transition class I . Waiting time distributions for blurred transitions can be interpreted as an average over all waiting time distributions for resolved transitions belonging to the corresponding transition classes. Thus, these waiting time distribution can be calculated via

$$\Psi_{I \rightarrow J}(t) = \sum_{\substack{(ij) \in I \\ (kl) \in J}} p(ij|I) \psi_{(ij)\rightarrow(kl)}(t), \quad (13)$$

using the corresponding weight from Eq. (12). The interpretation of $\Psi_{I \rightarrow J}(t)$ is similar to the interpretation of the waiting time distributions for resolved transitions defined in Eq. (8). Note that for the blurred observer, $p(ij|I)$ is not accessible because the individual transitions in a class are not distinguishable. Instead of using Eq. (13), this observer determines $\Psi_{I \rightarrow J}(t)$ directly from recorded histogram data for the corresponding transitions and waiting times.

Although the waiting time distributions for blurred transitions can be interpreted analogously to the waiting time distributions for resolved transitions, their meaning on the level of the underlying Markov network is significantly different. Directly after a transition from class I , the state of the underlying system can be the final state of any transition within I . For example, for the observation scenario shown in Fig. 3(a), right after a registered transition from class I , the state of the system is either two or five. In general, after a blurred transition, the state of the system is not fully determined, i.e., the state of the system is determined up to $p(ij|I)$. Thus, the effective dynamics on the level of blurred observations is non-Markovian at any point in time.

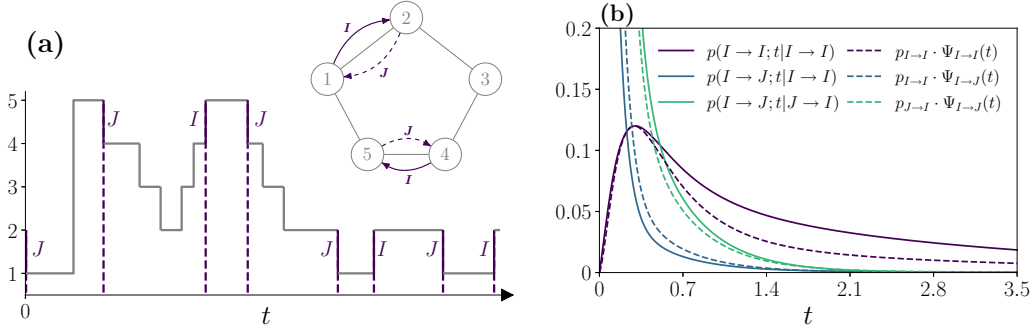


FIG. 3. Observation of a partially accessible five-state Markov network with two blurred transitions. (a) The blurred observer registers transitions from classes I and J and the corresponding in-between waiting times but cannot resolve the individual transitions within a class. (b) Breakdown of the renewal property, i.e., Eq. (15), for three out of eight possible sequences with three transitions. The deviations between the conditioned probabilities, e.g., $p(I \rightarrow J; t|I \rightarrow I)$, and the corresponding products, e.g., $p_{I \rightarrow I} \Psi_{I \rightarrow J}(t)$, indicate that the observed transitions are not Markovian. The probabilities and waiting time distributions are calculated with an absorbing master equation for transition rates $k_{12} = 0.4$, $k_{21} = 8.9$, $k_{23} = 4.2$, $k_{32} = 1.1$, $k_{34} = 1.8$, $k_{43} = 0.01$, $k_{45} = 9.4$, $k_{54} = 0.1$, $k_{51} = 8.8$, and $k_{15} = 0.6$.

From the perspective of the blurred observer, this breakdown of the renewal property leads to nonfactorizing waiting time distributions, e.g., for the sequence $I \rightarrow J \rightarrow K$ with waiting times t_1 and t_2 ,

$$\Psi_{I \rightarrow J \rightarrow K}(t_1, t_2) \neq \Psi_{I \rightarrow J}(t_1) \Psi_{J \rightarrow K}(t_2). \quad (14)$$

To illustrate Eq. (14) with the two-transition waiting time distributions of the example in Fig. 3(a), we integrate both sides over t_1 leading to

$$p(J \rightarrow K; t|I \rightarrow J) \neq p_{I \rightarrow J} \Psi_{J \rightarrow K}(t), \quad (15)$$

where

$$p_{I \rightarrow J} = \int_0^\infty dt \Psi_{I \rightarrow J}(t) \quad (16)$$

is the probability to observe a transition from class J after a transition from class I irrespective of the in-between waiting time. For the three different sequences with three transitions shown in Fig. 3(b), the renewal property breaks down.

The mapping from resolved transitions to blurred transitions is a time-independent, unique and many-to-one coarse-graining scheme for an already effective description of a partially accessible Markov network by the resolved observer. In the space of observable transitions, this coarse-graining scheme corresponds to lumping effective transition states into effective compound transition states. Crucially, although this strategy is similar to conventional coarse-graining by state lumping [7,10,11,15], the behavior of the resulting coarse-grained states under time-reversal is different. If we first apply the time-reversal operation for transitions and blur them into classes afterwards [36,37,39], the blurred transitions of a specific transition class can be even, odd or neither one under time-reversal. We adopt this notion also for the corresponding transition classes, i.e., the lumped states in the space of observable transitions. A transition class G is even under time-reversal if the time-reversed transition of each transition in G is also included in G . A transition class I is odd under time-reversal if the time-reversed transition of each transition in I is included in the time-reversed class \tilde{I} . For all other scenarios, the corresponding transition class is neither even nor odd. Note that this notion emphasizes

the difference between lumped transition states and conventional lumped states. The latter are always even under time-reversal.

As an example, consider again the system shown in Fig. 3(a). The transition classes $I = \{(12), (45)\}$ and $J = \{(21), (54)\}$ are odd transition classes, i.e., $\tilde{I} = J$ and $\tilde{J} = I$ because the time-reversed counterparts of the transitions in I are blurred into J . In contrast, blurring the resolved transitions into $G = \{(12), (21)\}$ and $H = \{(45), (54)\}$ would result in even transition classes, i.e., $\tilde{G} = G$ and $\tilde{H} = H$ because the time-reversed counterparts of the transitions in G and H would also be blurred into G and H , respectively. If the transitions were blurred into $K = \{(12), (21), (45)\}$ and $L = \{(54)\}$, the time-reversed transition classes $\tilde{K} = \{(21), (12), (54)\}$ and $\tilde{L} = \{(45)\}$ would not be observable and these transition classes would be neither even nor odd under time-reversal. In the following, we assume that for each transition class the corresponding time-reversed one is observable, i.e., we consider only even or odd transition classes.

IV. ESTIMATION OF ENTROPY PRODUCTION

Extending the analogy between waiting time distributions of resolved transitions and blurred transitions to the entropy estimator $\langle \hat{\sigma} \rangle$ leads to a generalization of Eq. (9) for blurred transitions given by

$$\langle \hat{\sigma}_{\text{BT}} \rangle \equiv \sum_{I,J} \int_0^\infty dt \pi_I \Psi_{I \rightarrow J}(t) \ln \frac{\Psi_{I \rightarrow J}(t)}{\Psi_{\tilde{J} \rightarrow \tilde{I}}(t)}, \quad (17)$$

where the summation includes all transition classes. Crucially, $\langle \hat{\sigma}_{\text{BT}} \rangle$ is not a bound for $\langle \sigma \rangle$, i.e., $\langle \hat{\sigma}_{\text{BT}} \rangle \not\leq \langle \sigma \rangle$ in general, because the entropy estimator for trajectory snippets is not applicable if no renewal events are observed. More specifically, the start and the end of the snippets are then not Markovian events, which breaks the central condition for applying the fluctuation theorem used for deriving $\langle \hat{\sigma} \rangle$ for resolved transitions [39,48]. To derive a waiting time based bound for blurred transitions, we start from Eq. (17) and insert the definition of the waiting time distributions from Eq. (13). By rewriting the conditioned probabilities using the definition

in Eq. (12), we can separate terms in Eq. (17) and apply the log-sum inequality from information theory [69] which leads to

$$\begin{aligned} \langle \hat{\sigma}_{\text{BT}} \rangle + \sum_{I,J} \pi_I p_{I \rightarrow J} \log \frac{\pi_I}{\pi_{\tilde{J}}} \\ \leq \sum_{I,J} \sum_{\substack{(ij) \in I \\ (kl) \in J}} \int_0^\infty dt \pi_{ij} \psi_{(ij) \rightarrow (kl)}(t) \ln \frac{\pi_{ij} \psi_{(ij) \rightarrow (kl)}(t)}{\pi_{\tilde{kl}} \psi_{(\tilde{kl}) \rightarrow (\tilde{ij})}(t)}. \end{aligned} \quad (18)$$

$$\langle \hat{\sigma}_{\text{BT}} \rangle + \sum_{I,J} \pi_I p_{I \rightarrow J} \log \frac{\pi_I}{\pi_{\tilde{J}}} \leq \sum_{I,J} \sum_{\substack{(ij) \in I \\ (kl) \in J}} \int_0^\infty dt (\pi_{ij} \psi_{(ij) \rightarrow (kl)}(t) - \pi_{\tilde{kl}} \psi_{(\tilde{kl}) \rightarrow (\tilde{ij})}(t)) \ln \frac{\pi_{ij} \psi_{(ij) \rightarrow (kl)}(t)}{\pi_{\tilde{kl}} \psi_{(\tilde{kl}) \rightarrow (\tilde{ij})}(t)} \quad (19)$$

$$\leq \sum_{(ij) \leq (kl)} \int_0^\infty dt (\pi_{ij} \psi_{(ij) \rightarrow (kl)}(t) - \pi_{\tilde{kl}} \psi_{(\tilde{kl}) \rightarrow (\tilde{ij})}(t)) \ln \frac{\pi_{ij} \psi_{(ij) \rightarrow (kl)}(t)}{\pi_{\tilde{kl}} \psi_{(\tilde{kl}) \rightarrow (\tilde{ij})}(t)} \quad (20)$$

$$= \sum_{(ij),(kl)} \int_0^\infty dt \pi_{ij} \psi_{(ij) \rightarrow (kl)}(t) \ln \frac{\psi_{(ij) \rightarrow (kl)}(t)}{\psi_{(\tilde{kl}) \rightarrow (\tilde{ij})}(t)} + \sum_{(ij),(kl)} \pi_{ij} p_{(ij) \rightarrow (kl)} \ln \frac{\pi_{ij}}{\pi_{\tilde{kl}}}. \quad (21)$$

In the first line, the summation index $(ij) \in I \leq (kl) \in J$ means that each pair of resolved transitions is counted once and that the pairs for which the same transition is observed two times, i.e., $(ij) \rightarrow (ij)$, are included. For deducing the inequality in the second line, we have to distinguish two cases. First, the summation in the first line may already include all pairs of resolved transitions in which case the second line is an equality. Second, a pair of resolved transitions may not be included in this summation if $\tilde{J} = I$ and $\tilde{I} = J$ holds for the transition classes of these transitions because the corresponding term in Eq. (17) then vanishes. However, the term for this pair of resolved transitions can still be added to the right-hand side of the first line since this term is positive due to $(a-b) \ln a/b \geq 0$ for $a, b \geq 0$. In both cases, the summation in the second line then includes all pairs of resolved transitions. For the third line, we have first rearranged the summation and then separated the contributions of the waiting time distributions from those of the probabilities. For the latter, we have also carried out the integration over the waiting times.

After identifying the waiting time contributions as $\langle \hat{\sigma} \rangle$ based on the definition in Eq. (9) and introducing the abbreviations

$$\langle \hat{\sigma}_{\text{TC}} \rangle = \sum_{I,J} \pi_I p_{I \rightarrow J} \log \frac{\pi_I}{\pi_{\tilde{J}}} \quad (22)$$

and

$$\langle \hat{\sigma}_{\text{RT}} \rangle = \sum_{(ij),(kl)} \pi_{ij} p_{(ij) \rightarrow (kl)} \ln \frac{\pi_{ij}}{\pi_{\tilde{kl}}}, \quad (23)$$

we obtain from Eq. (21) the inequality

$$\langle \hat{\sigma}_{\text{BT}} \rangle + \langle \hat{\sigma}_{\text{TC}} \rangle \leq \langle \hat{\sigma} \rangle + \langle \hat{\sigma}_{\text{RT}} \rangle. \quad (24)$$

Note that from a conceptual point of view, the difference $\langle \hat{\sigma}_{\text{RT}} \rangle - \langle \hat{\sigma}_{\text{TC}} \rangle$ is related to the entropy of the randomness associated with the different resolved transitions contributing

For identifying $\pi_I p_{I \rightarrow J}$ in the separated term, we have first carried out the integration over all waiting times in this term and have then used Eqs. (13) and (16). Note that since we only consider transition classes which are either even or odd under time-reversal, the summation on the right-hand side of the inequality includes the time-reversed partner of each resolved transition. Therefore, we can rewrite Eq. (18) as

to a blurred transition. As shown in Refs. [7,10,14], similar terms also emerge for conventional state-lumping.

Since we aim at deriving a bound for the full entropy production $\langle \sigma \rangle$ based on Eq. (24), we have to bound $\langle \hat{\sigma}_{\text{RT}} \rangle$ because $\langle \hat{\sigma} \rangle$ is always smaller than $\langle \sigma \rangle$. If the underlying Markov network is unicyclic, we plug in Eq. (10) and note that

$$\langle \hat{\sigma}_{\text{RT}} \rangle = j_c \sum_{(ij),(kl)} \ln \frac{\pi_{ij}}{\pi_{\tilde{kl}}} \leq j_c \mathcal{A}_c = \langle \sigma \rangle \quad (25)$$

holds true because we can always complete this summation to Eq. (2) by adding $(\pi_{ij} - \pi_{ji}) \ln \pi_{ij}/\pi_{ji} = j_c \ln \pi_{ij}/\pi_{ji} \geq 0$ and canceling the steady state probabilities [47]. If the underlying network is multicyclic, we reorder the summation in $\langle \hat{\sigma}_{\text{RT}} \rangle$, which leads to

$$\langle \hat{\sigma}_{\text{RT}} \rangle = \sum_{(ij),(kl)} (\pi_{ij} p_{(ij) \rightarrow (kl)} - \pi_{\tilde{kl}} p_{(\tilde{kl}) \rightarrow (\tilde{ij})}) \ln \pi_{ij}. \quad (26)$$

Using the normalization of $p_{(ij) \rightarrow (kl)}$ and exploiting the stationarity of the NESS, we can rewrite Eq. (26) as

$$\langle \hat{\sigma}_{\text{RT}} \rangle = \sum_{(ij)} (\pi_{ij} - \pi_{\tilde{ij}}) \ln \pi_{ij} \leq \langle \sigma \rangle, \quad (27)$$

where we have bounded $\langle \hat{\sigma}_{\text{RT}} \rangle$ by comparing this expression to the definition of $\langle \sigma \rangle$ in Eq. (1) and noting that we can always complete the summation by adding $(\pi_{ij} - \pi_{ji}) \ln \pi_{ij}/\pi_{ji} \geq 0$. Equation (27) is saturated if all transitions are observed or if $(\pi_{ij} - \pi_{ji}) \ln \pi_{ij}/\pi_{ji} = 0$ holds true for all unobserved transitions.

With $\langle \hat{\sigma}_{\text{RT}} \rangle \leq \langle \sigma \rangle$ for unicyclic and multicyclic networks, Eq. (24) reduces to our main result

$$\langle \hat{\sigma}_{\text{BT}} \rangle + \langle \hat{\sigma}_{\text{TC}} \rangle \leq 2 \langle \sigma \rangle, \quad (28)$$

which is a bound for the full entropy production of partially accessible Markov networks based on the observation of

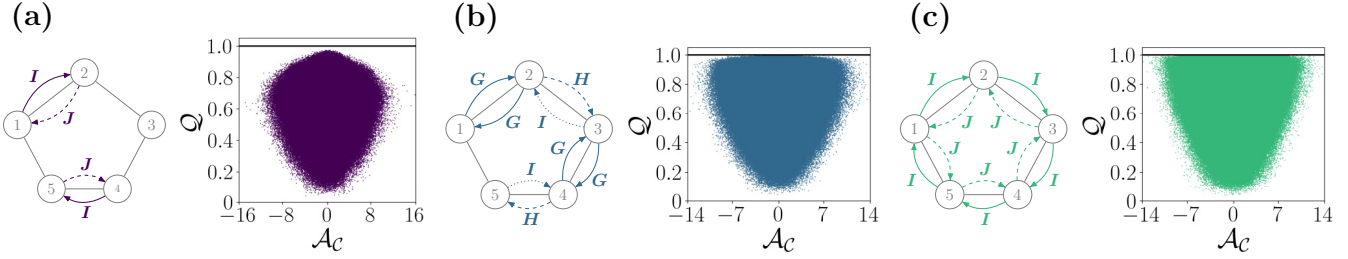


FIG. 4. Quality of the entropy bound in Eq. (28) for a unicyclic five-state Markov network as a function of the cycle affinity for three different observation scenarios. (a) Observation of the odd transition classes $I = \{(12), (45)\}$ and $J = \{(21), (54)\}$. The mean quality factor is given by $Q \simeq 0.66$. (b) Observation of the even transition class $G = \{(12), (21), (34), (43)\}$ and of the odd transition classes $H = \{(23), (45)\}$ and $I = \{(32), (54)\}$. The mean quality factor is given by $Q \simeq 0.77$. (c) Observation of the odd transition classes I and J including all forward and backward transitions, respectively. The mean quality factor is given by $Q \simeq 0.8$. Each scenario includes more than 4 000 000 network realizations with transition rates that are randomly drawn from uniform distributions between 0.1 and 6. All waiting time distributions are calculated with an absorbing master equation and Eq. (13).

blurred transitions. This bound can be used as operationally accessible entropy estimator because all quantities entering $\langle \hat{\sigma}_{\text{BT}} \rangle$ and $\langle \hat{\sigma}_{\text{TC}} \rangle$ are accessible in a blurred observation. Note that if each transition class includes only one transition, i.e., no transitions are blurred, both sides of Eq. (24) are equal, i.e., if $\langle \hat{\sigma}_{\text{BT}} \rangle = \langle \hat{\sigma} \rangle$ and $\langle \hat{\sigma}_{\text{TC}} \rangle = \langle \hat{\sigma}_{\text{RT}} \rangle$. If the observation additionally contains all transitions of the network, the bound in Eq. (28) is saturated because then $\langle \hat{\sigma} \rangle = \langle \sigma \rangle$ and $\langle \hat{\sigma}_{\text{RT}} \rangle = \langle \sigma \rangle$ hold true.

V. ILLUSTRATIONS

We illustrate our results with concrete observation scenarios for four different networks and with the observation scenario for the Schlögl model illustrated in Fig. 1. To quantify the quality of the bound in Eq. (28), we introduce the quality factor

$$Q \equiv \frac{\langle \hat{\sigma}_{\text{BT}} \rangle + \langle \hat{\sigma}_{\text{TC}} \rangle}{2 \langle \sigma \rangle} \leq 1. \quad (29)$$

We additionally introduce the abbreviation

$$\Sigma_{\text{BT}} \equiv \frac{\langle \hat{\sigma}_{\text{BT}} \rangle + \langle \hat{\sigma}_{\text{TC}} \rangle}{2} \leq \langle \sigma \rangle \quad (30)$$

for the entropy estimator derived in Eq. (28).

A. Unicyclic networks

We consider three different scenarios for the observation of the unicyclic five-state network from Fig. 3 shown in Fig. 4. For the observation scenario shown in Fig. 4(a), transitions of two different links are blurred into the odd transition classes I and J . For randomly drawn transition rates, the scatter plot shows that $Q < 1$ for any drawn affinity \mathcal{A}_C . In this simulation, the bound is never saturated because only four of ten transitions of the underlying network are observed. Even if Eq. (24) is saturated, the inequality in Eq. (25) is only saturated for a small set of rates with high symmetry, e.g., for $k_{23} = k_{32}, k_{34} = k_{43}, k_{51} = k_{15}$, which are unlikely to be drawn randomly. In the modified scenario shown in Fig. 4(b), transitions of three different links are blurred into the even transition class G and into the odd transition classes H and I . The scatter plot shows that $Q \leq 1$. Compared to the scenario in Fig. 4(a), the quality of the bound increases

because only the transitions (51) and (15) are not observed implying that Eq. (25) can be saturated for a larger set of rates, e.g., for $k_{51} = k_{15}$, which are more likely to be drawn randomly. In the observation scenario shown in Fig. 4(c), all forward transitions are blurred into the odd transition class I and all backward transitions are blurred into the odd transition class J . Since this observation includes all transitions of the network on the resolved level, i.e., $\langle \hat{\sigma}_{\text{RT}} \rangle = \langle \sigma \rangle$, the bound can be saturated for all rates that saturate Eq. (24).

B. Multicyclic networks

We consider the observation of three different multicyclic networks shown in Figs. 5(a)–5(c). The networks in Figs. 5(a) and 5(b) have multiple channels for the transitions (12) and (21). For each network, all transitions are observed on the resolved level and the forward and backward transitions of each link or each channel are blurred into a single even transition class. The corresponding scatter plots show that Q as a function of the average cycle affinity $\bar{\mathcal{A}}_C = \sum c_i \mathcal{A}_{c_i} / (\# \text{ cycles})$, i.e., the sum of all cycle affinities divided by the number of cycles, is always smaller than one or equal to one.

The mean quality factors for the observation in Fig. 5(a), $Q \simeq 0.06$, in Fig. 5(b), $Q \simeq 0.67$, and in Fig. 5(c), $Q \simeq 1.0$, are significantly different indicating distinct quality regimes of the bound. Since, as previously mentioned, the bound is saturated if no transitions are blurred, i.e., if each registered transition determines the state of the underlying system completely, one possible explanation for this result is the different degree of non-Markovianity of the considered scenarios. In the scenario shown in Fig. 5(a), each registered blurred transition is non-Markovian because each pair of subsequent transition classes has two possible realizations on the level of resolved transitions. In contrast, in the scenario shown in Fig. 5(b), registering the blurred transitions $I \rightarrow J$ or $J \rightarrow I$ corresponds to a Markovian event because, due to the topology of the network, the only possible resolved transition sequences for $I \rightarrow J$ and $J \rightarrow I$ are $(13) \rightarrow (32)$ and $(23) \rightarrow (31)$, respectively. Generalizing this argumentation to the scenario in Fig. 5(c), the bound in Eq. (28) is then saturated because for this network topology, each observed blurred transition corresponds to one unique transition registered by the resolved observer. Thus, each

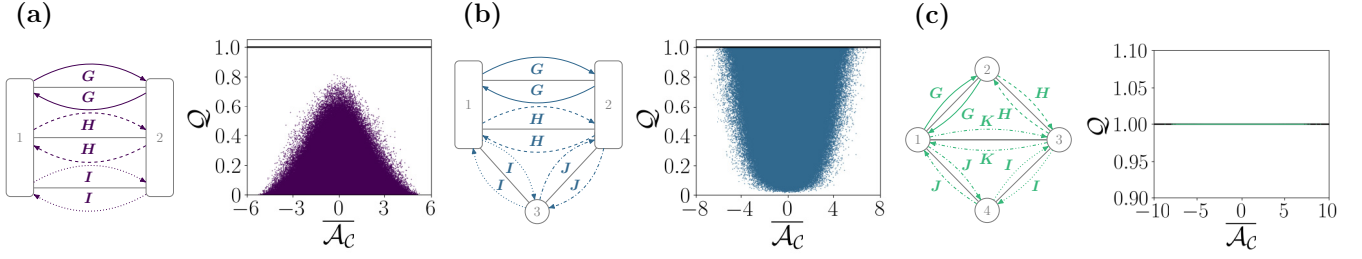


FIG. 5. Quality of the entropy bound in Eq. (28) for the observation of three multicyclic Markov network as a function of the average cycle affinity $\bar{\mathcal{A}}_C$. For each link, the forward and backward transitions are blurred into the same transition class. (a) Observation of a three channel network with even transition classes I, J and K . The mean quality factor is given by $Q \simeq 0.06$. (b) Observation of a three state network with two channels and even transition classes G, H, I, J , and K . The mean quality factor is given by $Q \simeq 0.67$. (c) Observation of a four state network with even transition classes G, H, I, J , and K . The mean quality factor is given by $Q \simeq 1.0$. Each observation includes more than 1 300 000 network realizations with transition rates that are randomly drawn from uniform distributions between 0.1 and 6. All waiting time distributions are calculated with an absorbing master equation and Eq. (13).

observed blurred transition is a Markovian event and the full $\langle \sigma \rangle$ is recovered in such a scenario where transitions of all links are observed without resolving their directionality.

C. Schlögl model

We consider the blurred observation of the Schlögl model as introduced in Fig. 1. Following the reaction scheme [51–53]



where k_{\pm}^A and k_{\pm}^B are the forward and backward transition rates of the A-reaction channel and the B-reaction channel, respectively, X molecules contained in an open system with size Ω can undergo chemical reactions with A and B molecules provided by two external reservoirs at fixed concentrations c_A and c_B . By the laws of mass-action kinetics, the transition rates of these reactions are determined by molecular rate constants via

$$k_+^A(n_X) = \kappa_+^A c_A \frac{n_X(n_X - 1)}{\Omega}, \quad (33)$$

$$k_-^A(n_X) = \kappa_-^A \frac{n_X(n_X - 1)(n_X - 2)}{\Omega^2}, \quad (34)$$

$$k_+^B(n_X) = \kappa_+^B c_B \Omega, \quad (35)$$

$$k_-^B(n_X) = \kappa_-^B n_X, \quad (36)$$

where n_X is the number of X molecules.

We assume that the system is out of equilibrium due to a difference in chemical potential $\Delta\mu = \mu_B - \mu_A$ between the two chemical reservoirs. For thermodynamic consistency, we require that the local detailed balance condition

$$\Delta\mu = \ln \frac{c_A \kappa_+^A \kappa_-^B}{c_B \kappa_-^A \kappa_+^B} \quad (37)$$

holds true. By transforming one A molecule into one B molecule via the creation and depletion of one X molecule, the system completes a cycle with affinity $\Delta\mu$. These cycle

completions lead to a nonvanishing mean entropy production rate

$$\langle \sigma \rangle = j_X \Delta\mu, \quad (38)$$

where j_X is the mean current of molecules entering and leaving the two reservoirs.

Following the observation scenario in Fig. 1, we assume that an external observer with no access to n_X aims at inferring $\langle \sigma \rangle$ based on the observation of the different reaction types ($A \rightarrow$), ($A \leftarrow$), ($B \rightarrow$), and ($B \leftarrow$). As shown in Fig. 6, the bound in Eq. (28) saturates within numerical errors for all considered concentrations c_A and system sizes Ω which implies that the estimator Σ_{BT} recovers the full entropy production of the system for these parameters.

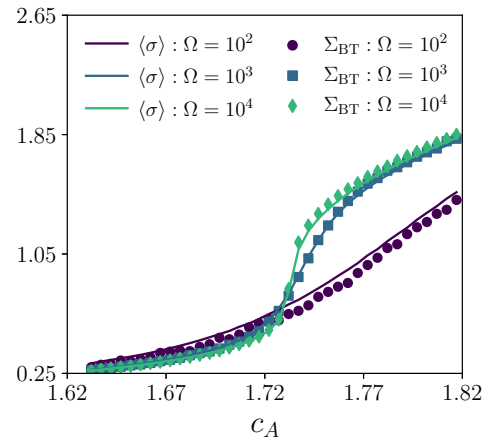


FIG. 6. Entropy production rate $\langle \sigma \rangle$ and entropy estimator Σ_{BT} for the blurred observation of the Schlögl model as a function of c_A at different system sizes Ω with $\Delta\mu = \ln 9$ and $\kappa_{\pm}^{A/B} = 1$. The stationary distribution of n_X needed for calculating the waiting time distributions via Eq. (13) is estimated numerically based on Gillespie simulation data. The slight deviations between $\langle \sigma \rangle$ and Σ_{BT} emerge as a consequence of the numerical error of the estimation method for the stationary distribution and as a consequence of the finite sample size. The increase in $\langle \sigma \rangle$ at $c_A \simeq 1.73$ is caused by the phase transition of the Schlögl model at the critical point [52,53].

This numerical result can be rationalized by comparing the amount of information accessible for the blurred observer to the amount of information contained in $\langle\sigma\rangle$ in Eq. (38). Although the effective Markov network for the resolved observation of the Schlögl model illustrated in Fig. 1(b) is multicyclic, Eq. (38) does not resolve each cycle of the network individually because, due to symmetry, all cycles of the network have the same affinity $\Delta\mu$. Furthermore, j_X is independent of resolving individual cycles because this current recovers the average number of created and consumed A and B molecules of the whole network. Conceptually, the same amount of information is included in Σ_{BT} . Each blurred transition corresponds to the creation or the consumption of one A or one B molecule recovering the information contained in j_X . Additionally, as shown in general and illustrated for the Brusselator model in Ref. [66], the probabilities for specific blurred transition sequences, for example $(A \rightarrow) \rightarrow (B \leftarrow)$ or $(A \leftarrow) \rightarrow (B \rightarrow)$, recover the cycle affinity $\Delta\mu$. Thus, the blurred observation captures the information contained in $\langle\sigma\rangle$ implying the saturation of the corresponding entropy bound.

VI. CONCLUSION

In this paper, we have extended the transition-based description of partially accessible Markov networks to those with blurred transitions by introducing the concept of transition classes. To establish an effective description from the perspective of such a blurred observer, we have introduced waiting time distributions for transitions between transition classes. Based on these waiting time distributions, we have demonstrated that this effective description is in general non-Markovian, i.e., does not include any renewal event. As a

consequence, the extant entropy estimator from Ref. [39] defined for resolved observed transition is not applicable. As this result implies that the formulation of any direct waiting time based entropy estimator most likely will fail, we have proven a complementary bound based on the log-sum inequality which reduces to an operationally accessible entropy estimator. Furthermore, we have illustrated the operational relevance of this estimator with various examples.

Future work could address the following issues. So far, the effective description is formulated for partially accessible Markov networks, which implies that its range of applicability is restricted to discrete systems. Generalizing the concept of transition classes to continuous degrees of freedom is therefore a possible next step. This generalization could additionally lead to an entropy estimator for the continuous analog of blurred transitions. Similarly, the description can potentially be generalized to systems which are not in a NESS, for example to systems with time-dependent driving. Our coarse-graining procedure leads to another open question. As state lumping is only one established coarse-graining scheme out of many, the extension of other schemes to the space of observable transitions might be possible as well. Assuming that these extensions lead to analogous bounds with a different range of validity, it might be possible to infer the realized coarse-graining in an observed systems based on the saturation or violation of the respective bounds.

ACKNOWLEDGMENTS

We thank Julius Degünther and Benedikt Remlein for fruitful discussions, the latter for providing raw simulation data for the Schlögl model, and Jann van der Meer for insightful discussions and a crucial moment of inspiration.

-
- [1] K. Sekimoto, *Stochastic Energetics*, Lecture Notes in Physics (Springer, Berlin, 2010).
 - [2] C. Jarzynski, Equalities and inequalities: Irreversibility and the second law of thermodynamics at the nanoscale, *Annu. Rev. Condens. Matter Phys.* **2**, 329 (2011).
 - [3] U. Seifert, Stochastic thermodynamics, fluctuation theorems and molecular machines, *Rep. Prog. Phys.* **75**, 126001 (2012).
 - [4] T. Schmiedl and U. Seifert, Stochastic thermodynamics of chemical reaction networks, *J. Chem. Phys.* **126**, 044101 (2007).
 - [5] H. Ge, M. Qian, and H. Qian, Stochastic theory of nonequilibrium steady states. Part II: Applications in chemical biophysics, *Phys. Rep.* **510**, 87 (2012).
 - [6] R. Rao and M. Esposito, Nonequilibrium thermodynamics of chemical reaction networks: Wisdom from stochastic thermodynamics, *Phys. Rev. X* **6**, 041064 (2016).
 - [7] M. Esposito, Stochastic thermodynamics under coarse graining, *Phys. Rev. E* **85**, 041125 (2012).
 - [8] J. Mehl, B. Lander, C. Bechinger, V. Blickle, and U. Seifert, Role of hidden slow degrees of freedom in the fluctuation theorem, *Phys. Rev. Lett.* **108**, 220601 (2012).
 - [9] M. Uhl, P. Pietzonka, and U. Seifert, Fluctuations of apparent entropy production in networks with hidden slow degrees of freedom, *J. Stat. Mech.* (2018) 023203.
 - [10] S. Bo and A. Celani, Multiple-scale stochastic processes: Decimation, averaging, and beyond, *Phys. Rep.* **670**, 1 (2017).
 - [11] S. Rahav and C. Jarzynski, Fluctuation relations and coarse-graining, *J. Stat. Mech.* (2007) P09012.
 - [12] A. Gomez-Marin, J. M. R. Parrondo, and C. Van den Broeck, Lower bounds on dissipation upon coarse graining, *Phys. Rev. E* **78**, 011107 (2008).
 - [13] A. Puglisi, S. Pigolotti, L. Rondoni, and A. Vulpiani, Entropy production and coarse graining in Markov processes, *J. Stat. Mech.* (2010) P05015.
 - [14] S. Bo and A. Celani, Entropy production in stochastic systems with fast and slow time-scales, *J. Stat. Phys.* **154**, 1325 (2014).
 - [15] D. Seiferth, P. Sollich, and S. Klumpp, Coarse graining of biochemical systems described by discrete stochastic dynamics, *Phys. Rev. E* **102**, 062149 (2020).
 - [16] E. Roldán and J. M. R. Parrondo, Estimating dissipation from single stationary trajectories, *Phys. Rev. Lett.* **105**, 150607 (2010).

- [17] E. Roldán and J. M. R. Parrondo, Entropy production and Kullback-Leibler divergence between stationary trajectories of discrete systems, *Phys. Rev. E* **85**, 031129 (2012).
- [18] N. Shiraishi and T. Sagawa, Fluctuation theorem for partially masked nonequilibrium dynamics, *Phys. Rev. E* **91**, 012130 (2015).
- [19] M. Poletini and M. Esposito, Effective thermodynamics for a marginal observer, *Phys. Rev. Lett.* **119**, 240601 (2017).
- [20] G. Bisker, M. Poletini, T. R. Gingrich, and J. M. Horowitz, Hierarchical bounds on entropy production inferred from partial information, *J. Stat. Mech.* (2017) 093210.
- [21] A. C. Barato and U. Seifert, Thermodynamic uncertainty relation for biomolecular processes, *Phys. Rev. Lett.* **114**, 158101 (2015).
- [22] T. R. Gingrich, J. M. Horowitz, N. Perunov, and J. L. England, Dissipation bounds all steady-state current fluctuations, *Phys. Rev. Lett.* **116**, 120601 (2016).
- [23] P. Pietzonka, A. C. Barato, and U. Seifert, Universal bounds on current fluctuations, *Phys. Rev. E* **93**, 052145 (2016).
- [24] R. Marsland, W. Cui, and J. M. Horowitz, The thermodynamic uncertainty relation in biochemical oscillations, *J. R. Soc. Interface* **16**, 20190098 (2019).
- [25] J. M. Horowitz and T. R. Gingrich, Thermodynamic uncertainty relations constrain non-equilibrium fluctuations, *Nat. Phys.* **16**, 15 (2020).
- [26] P. Pietzonka and F. Coghi, Thermodynamic cost for precision of general counting observables, [arXiv:2305.15392](https://arxiv.org/abs/2305.15392) (2023).
- [27] G. Teza and A. L. Stella, Exact coarse graining preserves entropy production out of equilibrium, *Phys. Rev. Lett.* **125**, 110601 (2020).
- [28] J. Ehrlich, Tightest bound on hidden entropy production from partially observed dynamics, *J. Stat. Mech.* (2021) 083214.
- [29] D. J. Skinner and J. Dunkel, Improved bounds on entropy production in living systems, *Proc. Natl. Acad. Sci. USA* **118**, e2024300118 (2021).
- [30] E. Nitzan, A. Ghosal, and G. Bisker, Universal bounds on entropy production inferred from observed statistics, *Phys. Rev. Res.* **5**, 043251 (2023).
- [31] R. Elber, Milestoning: An efficient approach for atomically detailed simulations of kinetics in biophysics, *Annu. Rev. Biophys.* **49**, 69 (2020).
- [32] D. Hartich and A. Godec, Violation of local detailed balance upon lumping despite a clear timescale separation, *Phys. Rev. Res.* **5**, L032017 (2023).
- [33] A. M. Berezhkovskii and D. E. Makarov, On the forward/backward symmetry of transition path time distributions in nonequilibrium systems, *J. Chem. Phys.* **151**, 065102 (2019).
- [34] I. A. Martínez, G. Bisker, J. M. Horowitz, and J. M. R. Parrondo, Inferring broken detailed balance in the absence of observable currents, *Nat. Commun.* **10**, 3542 (2019).
- [35] D. Hartich and A. Godec, Emergent memory and kinetic hysteresis in strongly driven networks, *Phys. Rev. X* **11**, 041047 (2021).
- [36] D. Hartich and A. Godec, Comment on “Inferring broken detailed balance in the absence of observable currents,” [arXiv:2112.08978](https://arxiv.org/abs/2112.08978) (2021).
- [37] G. Bisker, I. A. Martínez, J. M. Horowitz, and J. M. R. Parrondo, Comment on “Inferring broken detailed balance in the absence of observable currents,” [arXiv:2202.02064](https://arxiv.org/abs/2202.02064) (2021).
- [38] D. J. Skinner and J. Dunkel, Estimating entropy production from waiting time distributions, *Phys. Rev. Lett.* **127**, 198101 (2021).
- [39] J. van der Meer, B. Ertel, and U. Seifert, Thermodynamic inference in partially accessible Markov networks: A unifying perspective from transition-based waiting time distributions, *Phys. Rev. X* **12**, 031025 (2022).
- [40] P. E. Harunari, A. Dutta, M. Poletini, and E. Roldán, What to learn from a few visible transitions’ statistics? *Phys. Rev. X* **12**, 041026 (2022).
- [41] X. Li and A. B. Kolomeisky, Mechanisms and topology determination of complex chemical and biological network systems from first-passage theoretical approach, *J. Chem. Phys.* **139**, 144106 (2013).
- [42] A. M. Berezhkovskii and D. E. Makarov, From nonequilibrium single-molecule trajectories to underlying dynamics, *J. Phys. Chem. Lett.* **11**, 1682 (2020).
- [43] A. L. Thorneywork, J. Gladrow, Y. Qing, M. Rico-Pasto, F. Ritort, H. Bayley, A. B. Kolomeisky, and U. F. Keyser, Direct detection of molecular intermediates from first-passage times, *Sci. Adv.* **6**, eaaz4642 (2020).
- [44] B. Ertel, J. van der Meer, and U. Seifert, Waiting time distributions in hybrid models of motor–bead assays: A concept and tool for inference, *Int. J. Mol. Sci.* **24**, 7610 (2023).
- [45] H. Wang and H. Qian, On detailed balance and reversibility of semi-Markov processes and single-molecule enzyme kinetics, *J. Math. Phys.* **48**, 013303 (2007).
- [46] C. Maes, K. Netočný, and B. Wynants, Dynamical fluctuations for semi-Markov processes, *J. Phys. A: Math. Theor.* **42**, 365002 (2009).
- [47] B. Ertel, J. van der Meer, and U. Seifert, Operationally accessible uncertainty relations for thermodynamically consistent semi-Markov processes, *Phys. Rev. E* **105**, 044113 (2022).
- [48] J. van der Meer, J. Degünther, and U. Seifert, Time-resolved statistics of snippets as general framework for model-free entropy estimators, *Phys. Rev. Lett.* **130**, 257101 (2023).
- [49] J. Degünther, J. van der Meer, and U. Seifert, Fluctuating entropy production on the coarse-grained level: Inference and localization of irreversibility, [arXiv:2309.07665](https://arxiv.org/abs/2309.07665) (2023).
- [50] A. Godec and D. E. Makarov, Challenges in inferring the directionality of active molecular processes from single-molecule fluorescence resonance energy transfer trajectories, *J. Phys. Chem. Lett.* **14**, 49 (2023).
- [51] F. Schlögl, Chemical reaction models for non-equilibrium phase transitions, *Z. Phys.* **253**, 147 (1972).
- [52] I. Matheson, D. F. Walls, and C. W. Gardiner, Stochastic models of firstorder nonequilibrium phase transitions in chemical reactions, *J. Stat. Phys.* **12**, 21 (1975).
- [53] M. Vellela and H. Qian, Stochastic dynamics and non-equilibrium thermodynamics of a bistable chemical system: The Schlögl model revisited, *J. R. Soc. Interface* **6**, 925 (2009).
- [54] B. Remlein and U. Seifert, Nonequilibrium fluctuations of chemical reaction networks at criticality: The Schlögl model as paradigmatic case, *J. Chem. Phys.* **160**, 134103 (2024).
- [55] J. S. van Zon, D. K. Lubensky, P. R. H. Altena, and P. R. ten Wolde, An allosteric model of circadian KaiC phosphorylation, *Proc. Natl. Acad. Sci. USA* **104**, 7420 (2007).

- [56] C. H. Johnson, P. L. Stewart, and M. Egli, The cyanobacterial circadian system: From biophysics to bioevolution, *Annu. Rev. Biophys.* **40**, 143 (2011).
- [57] J. Paijmans, D. K. Lubensky, and P. R. ten Wolde, Period robustness and entrainability of the Kai system to changing nucleotide concentrations, *Biophys. J.* **113**, 157 (2017).
- [58] B. Nguyen, U. Seifert, and A. C. Barato, Phase transition in thermodynamically consistent biochemical oscillators, *J. Chem. Phys.* **149**, 045101 (2018).
- [59] M. J. Schnitzer, Theory of continuum random walks and application to chemotaxis, *Phys. Rev. E* **48**, 2553 (1993).
- [60] J. Tailleur and M. E. Cates, Statistical mechanics of interacting run-and-tumble bacteria, *Phys. Rev. Lett.* **100**, 218103 (2008).
- [61] P. Pietzonka and U. Seifert, Entropy production of active particles and for particles in active baths, *J. Phys. A: Math. Theor.* **51**, 01LT01 (2018).
- [62] R. Sánchez, R. López, D. Sánchez, and M. Büttiker, Mesoscopic Coulomb drag, broken detailed balance, and fluctuation relations, *Phys. Rev. Lett.* **104**, 076801 (2010).
- [63] G. Bulnes Cuetara, M. Esposito, and P. Gaspard, Fluctuation theorems for capacitively coupled electronic currents, *Phys. Rev. B* **84**, 165114 (2011).
- [64] G. B. Cuetara and M. Esposito, Double quantum dot coupled to a quantum point contact: A stochastic thermodynamics approach, *New J. Phys.* **17**, 095005 (2015).
- [65] M. Borrelli, J. V. Koski, S. Maniscalco, and J. P. Pekola, Fluctuation relations for driven coupled classical two-level systems with incomplete measurements, *Phys. Rev. E* **91**, 012145 (2015).
- [66] P. E. Harunari, Unveiling nonequilibrium from multifilar events, [arXiv:2402.00837](https://arxiv.org/abs/2402.00837) (2024).
- [67] T. L. Hill, *Free Energy Transduction and Biochemical Cycle Kinetics* (Springer, New York, NY, 1989).
- [68] D.-Q. Jiang, M. Qian, and M.-P. Qian, *Mathematical Theory of Nonequilibrium Steady States* (Springer, Berlin, 2004).
- [69] T. M. Cover and J. A. Thomas, *Elements of Information Theory* (*Wiley Series in Telecommunications and Signal Processing*) (Wiley-Interscience, New York, NY, 2006).